

Mapping the DNA- and zinc-binding domains of ASR1 (abscisic acid stress ripening), an abiotic-stress regulated plant specific protein

Slava Rom^a, Ayelet Gilad^a, Yossi Kalifa^{a,1}, Zvia Konrad^a, Mark M. Karpasas^b,
Yehuda Goldgur^c, Dudy Bar-Zvi^{a,*}

^a Department of Life Sciences and Doris and Bertie Black Center for Bioenergetics in Life Sciences,
Ben-Gurion University of the Negev, P.O.B. 653, Beer-Sheva 84105, Israel

^b The Institutes for Applied Biosciences, Ben-Gurion University, Beer-Sheva, Israel

^c Department of Chemistry, Ben-Gurion University, Beer-Sheva 84105, Israel

Received 24 August 2005; accepted 21 November 2005

Available online 09 December 2005

Abstract

Abscisic acid stress ripening (ASR1) is a highly charged low molecular weight plant specific protein that is regulated by salt- and water-stresses. The protein possesses a zinc-dependent DNA-binding activity (Kalifa et al., *Biochem. J.* 381 (2004) 373) and overexpression in transgenic plants results in an increased salt-tolerance (Kalifa et al., *Plant Cell Environ.* 27 (2004) 1459). There are no structure homologs of ASR1, thus the structural and functional domains of the protein cannot be predicted. Here, we map the protein domains involved in the binding of Zn²⁺ and DNA. Using mild acid hydrolysis, and a series of ASR1 carboxy-terminal truncations we show that the zinc-dependent DNA-binding could be mapped to the central/carboxy-terminal domain. In addition, using MALDI-TOF-MS with a non-acidic matrix, we show that two zinc ions are bound to the amino-terminal domain. Other zinc ion(s) bind the DNA-binding domain. Binding of zinc to ASR1 induces conformational changes resulting in a decreased sensitivity to proteases.

© 2005 Elsevier SAS. All rights reserved.

Keywords: Abiotic-stress; DNA-binding; Salt-stress; Water-stress; Zinc-binding; Zinc-dependent DNA-binding

1. Introduction

Abscisic acid stress ripening (ASR1) is a highly charged low molecular weight protein whose expression is transiently induced by salt-stress, water-stress and by treatment with the plant hormone abscisic acid (ABA) [1]. A molecular mechanism for its biological role cannot be deduced simply by sequence homology with other known proteins. In tomato, *Asr1*

belongs to a small gene family [2–4], with homologs cloned from a variety of gymnosperm, monocot and dicot plant species (reviewed in [5]). Low levels of *Asr1* mRNA and its protein product were detected in roots and shoots of irrigated tomato plants [1]. Following NaCl, poly(ethylene glycol) (PEG) or ABA treatment these levels were transiently increased [1]. Transient expression of an ASR1 homolog was also observed in roots of salt stressed maize plants [6], and the rice ASR1 homolog was highly expressed following 3 and 6 hours exposure to excess salt in two rice varieties that differed in their salt-tolerance [7]. *Asr1* expression also appears to be developmentally regulated such that levels of *Asr1* mRNA increase during fruit ripening [2,8].

ASR1 homologs can be classified into four broad classes based on the primary amino acid sequence [9]. Three of these classes are composed of genes whose expression levels are increased by desiccation or salt-stress (e.g. [6,10–12]), whereas

Abbreviations: ABA, abscisic acid; ASR1, abscisic acid stress ripening; HCCA, 4-hydroxy- α -cyanocinnamic acid; Hepes, N-2-hydroxyethylpiperazine-N'-2-ethanesulfonic acid; PEG, poly(ethylene glycol); TCA, trichloroacetic acid; TFA, trifluoroacetic acid; THAP, 2',4',6'-trihydroxy-acetophenone.

* Corresponding author. Tel.: +972 8 646 1365; fax: +972 8 647 9198.

E-mail address: barzvi@bgu.ac.il (D. Bar-Zvi).

¹ Present address: Department of Molecular Biology, Princeton University, Princeton, NJ 08544, USA.

the fourth class contains cDNAs cloned from fruit tissues (e.g. [13–15]).

A molecular biological role for ASR1 has been recently suggested: tomato ASR1 was shown to possess Zn²⁺-dependent DNA-binding activity [16] and overexpression of tomato ASR1 in transgenic tobacco plants increases their salt-tolerance [17]. VvMSA, a grape ASR homolog from the fruit specific subclass, was shown to bind DNA and proposed to modulate the expression of sugar-regulated genes [15].

DNA-binding proteins have been classified into eight groups according to the structure of the DNA-bound protein and the overall pattern of DNA recognition (reviewed in [18]). The helix–turn helix (HTH) motif is common in enzymes and transcription factors from both prokaryotic and eukaryotic organisms [19]. Zipper-type proteins, described based on their dimerization mechanism, include the leucine zipper family and the helix–loop–helix–leucine zipper family [20,21]. Other groups include the α -helix proteins, β -sheet proteins, β -hairpin/ribbon proteins, and DNA-binding enzymes [18]. The largest group of eukaryotic transcription factors, namely the zinc finger proteins, contains zinc ions as described below.

Zinc is an essential cofactor and is bound by proteins through coordination by the amino acids His, Asp, Glu and Cys, and water molecules. Zinc-binding sites have been classified depending on whether they form part of a catalytic domain or perform a structural role in stabilizing the tertiary structure. In the former, zinc ions are usually complexed by three amino acid residues and a water molecule, whereas in the latter, zinc is coordinated exclusively by four amino acids [22]. His is the most common residue for zinc-binding in catalytic sites; Cys is preferred in non-catalytic sites. Zinc-binding also plays a role in cocatalytic sites and protein interfaces, and as described in a recent review [22] more than one zinc ion may be involved in these cases.

Zinc containing DNA-binding proteins can be divided into four subgroups; of which the $\beta\beta\alpha$ zinc-finger family is the largest [23]. In fact, the zinc-finger DNA-binding proteins represent the best studied group of the structural zinc proteins. The finger structure is characterized by two short stranded antiparallel β sheets followed by a α -helix, held together by the coordination of a single zinc ion via two pairs of Cys and Cys or His residues. Proteins of the zinc finger family play an important role in development and often contain multiple fingers that bind a DNA target. For example, zinc fingers of the Cys–Cys class in which a single zinc ion is coordinated by four Cys residues include the GATA [24] and hormone receptor families: the steroid and thyroid hormones are soluble proteins that translocate between cytoplasm and nucleus in response to ligand binding [25]. Other examples zinc-binding transcription factors include the loop–sheet–helix zinc coordinating protein family which bind zinc via 3 Cys and 1 His, such as the tumor suppressor p53 [26], and the cysteine-zinc cluster found in yeast Gal4 in which six Cys residues bind two zinc ions [27].

Although ASR1 possesses a zinc-dependent DNA-binding activity [16], it is not a zinc-finger protein since it lacks Cys residues. Furthermore, based on an analysis of the primary ASR sequence, it would appear as though the ASR proteins

do not have any known DNA-binding motifs (data not shown). In this study we mapped the DNA and zinc-binding domains of ASR1: DNA-binding was mapped to the carboxy half of the protein, based on peptide products obtained by mild acid hydrolysis and a series of carboxy-terminal truncations. The interaction of two zinc ions per ASR1 polypeptide was further demonstrated using MALDI-TOF-MS. The binding of zinc results in a concomitant decrease in sensitivity to proteases. Zinc-binding was mapped to the amino half of ASR1 protein.

2. Materials and methods

2.1. Plant material and extraction of leaf proteins

Tomato (*L. esculantum* Mill., cv. Ailsa Craig) plants were grown hydroponically in Hoagland's solution as described previously in [1]. Tomato leaves were homogenized in ice cold homogenization buffer at a tissue/buffer ratio of 1:5 (w/v), using a Polytron homogenizer (Kinematica, Luzern, Switzerland; 15 s pulses at full speed). Unless otherwise indicated, the homogenization buffer used was composed of 25 mM Hepes–NaOH pH 7.5, 10 mM MgCl₂, 0.5 M sucrose, 10 mM β -mercaptoethanol, and 0 or 1 mM ZnCl₂. The homogenate was filtered through four layers of Miracloth (Calbiochem, San Diego, CA, USA).

2.2. Construction of deletion mutants

ASR1 truncated proteins were obtained by mutating the codons encoding for amino acid residues 61, 69, 77, 87, 96 and 105 into stop codons. Mutated DNA sequences were synthesized by polymerase chain reaction using ASR11 forward primer (ATGACTAGTCCATGGAGGAGGAGAA) that introduces an *Nde*I restriction site (underlined) at the ATG start codon (bold), and one of the following reverse primers, introducing stop codons (bold) and an *Eco*RI restriction site (underlined): ASR60, AACTGAATTCAACTTTCTTTGCCTCATG; ASR68, AACTGAATTCACTTGTGTTTGTGTGCA TG; ASR76, AACTGAATTCCAAGCTGCTGCTATCTTCTT; ASR86, AACTGAATTCAGAAATGCAAATCCACCTG; ASR95, AACTGAATTCAGGCATCTTTTTTCTCATG; ASR104, AACTGAATTCACCTCAGCTTTTTTTTCT. Reaction mix contained in a final volume of 50 μ l 75 mM Tris–HCl pH 8.8, 20 mM (NH₄)₂SO₄, 0.01% Tween 20, 0.2 mM (each) dNTP, 20 pM of each primer, 25 ng ASR1 cDNA and 0.25 U Pfu DNA polymerase (Stratagene, La Jolla, CA, USA). Mutagenized DNA was synthesized by 35 cycles of 30 s at 95 °C, 45 s at 52 °C, and 45 s at 72 °C following by 5 min at 72 °C. Amplified DNA were digested with *Nde*I and *Eco*RI and subcloned into the appropriate sites in a pRSET B expression vector (Invitrogen).

2.3. Expression and purification of ASR1 and derivative proteins

Plasmids encoding full-length ASR1 and deletion derivatives were used to transform *E. coli* BL21 Codon Plus cells.

To express the ASR1 proteins, 0.4 mM IPTG was added to logarithmically growing *E. coli* cultures ($OD_{600\text{ nm}} = 0.4$). Cells were harvested 3 h later, washed twice in ice cold washing buffer (20 mM Tris–HCl pH 7), and resuspended in the same buffer containing complete, EDTA free, protease inhibitor cocktail (Roche). Cells were lysed by sonication, insoluble material was removed by centrifugation at $12,000 \times g$ for 15 min at 4 °C. Full length and derivative ASR1 proteins were purified from the supernatants as previously described in [16].

2.4. Mild acid hydrolysis

Mild acid hydrolysis was carried out using a modified published protocol [28]. Briefly, purified ASR1 was incubated in 0.3% (w:v) of trifluoroacetic acid (TFA) at 100 °C for 2 h. Ice cold trichloroacetic acid (TCA) was added to a final volume of 25% (w:v) and mixtures were incubated on ice for 15 min. Resulting polypeptides were precipitated by centrifugation at $12,000 \times g$ for 20 min at 4 °C. Pellets were washed twice in cold (–20 °C) acetone, dried, and resuspended in electrophoresis sample buffer [29].

2.5. DNA-binding

ASR1 proteins were resolved on SDS-PAGE, transferred onto a 0.2 μm nitrocellulose membrane, and assayed for DNA-binding by south-western analysis as previously described in [16]. Radiolabeled dsDNA ACTAGTGATTAA CAGCTATGACCATGAAGCTTATCCACT**CCCCATGATC** CACTAGTTCTAGAAATC containing the preferred ASR1 binding site (in bold) was used as a probe.

2.6. Protein electrophoresis

Protein SDS-PAGE was performed using the high-molarity Tris buffer system enabling a better resolution of low molecular weight polypeptides [29].

2.7. Western blot

ASR1 was detected immunologically using anti-tomato antiserum as previously described in [16,17].

2.8. Proteolysis

Mixtures containing 4 μg ASR1 in 20 Hepes–NaOH pH 7.5, 20 mM NaCl and the indicated ZnCl_2 concentrations in 60 μl were incubated for 10 min. Proteases were added, and tubes were incubated for 1 h at 37 °C. Proteases used: trypsin (0.2 μg), proteinase V8 (30 ng), proteinase K (12 ng) or chymotrypsin (12 μg). Proteolysis products were analyzed by SDS-PAGE or by MALDI-TOF-MS.

2.9. MALDI-TOF-MS

Mass spectrometric analysis was performed on a Bruker Reflex IV time-of-flight (TOF) mass spectrometer (Bruker Daltonics, Bremen, Germany). Ions were formed using a pulsed nitrogen laser operating at 337 nm. Mass spectra, obtained from the average of up to 350 single-shot spectra, were collected using an acceleration voltage of 25 kV and a delay of 150 ns.

Purified ASR1 or its derivatives were mixed with an equal volume of one of the following matrices: 1) non-acidic THAP matrix was prepared as 15 mg/ml 2',4',6'-trihydroxy-acetophenone in 50% acetonitrile in water; 2) non-acidic HCCA matrix was prepared by mixing a saturated solution of 4-hydroxy- α -cyanocinnamic acid (HCCA) in 1:1 mix (v:v) of 1 M ammonium bicarbonate (pH 8.0): ethanol [30]; 3) 2,5 dihydrobenzoic (DHB) acid in 33% (v/v) acetonitrile and 67% (v/v) 0.1% aqueous solution of TFA. All matrix reagents were of the highest available grade. Acids and organic solvents were of HPLC grade. 0.8- μl samples of the protein–matrix mixtures were applied to dry on AnchorChipTM 600 μm (Bruker). External protein standards (Bruker) were used for calibration.

To map the zinc-binding sites, ASR1 was digested by trypsin as previously described. Reactions were quenched by the addition of TFA (2–3% final concentration). Twenty microliters of reaction samples were dried by speed-vac, peptides were dissolved by sonication in 8 μl aqueous 5% acetonitrile plus 2% TFA solution. 1.5 μl of protein mix was mixed with equal volume of freshly prepared matrix obtained by mixing 2 vol of HCCA (Aldrich, Milwaukee, WI) dissolved in acetone: 1 vol of 20 mg/ml nitrocellulose (Transblot, Bio-Rad, Hercules, CA) dissolved in acetone: 1 vol isopropanol [31]. One microliter of this mixture was spotted onto the MALDI target and air dried. Immobilized samples were washed by 5 μl of 5% formic acid followed by Milli-Q water [31]. The spotted samples were placed into a Bruker Daltonics Reflex IV TOF instrument (Bremen, Germany). Five hundred shots per spectrum were collected and several spectra were accumulated if necessary. The data were then analyzed in Data Explorer (XTOF, version 5.1.5). The spectra were baseline corrected and peak detection parameters were set to label monoisotopic masses as appropriate for each sample. External peptide calibration standards (Bruker) were used. Peptides known to be from trypsin's autolysis [32] were omitted from the data file and Bruker Daltonics BioToolsTM 2.0. was used to obtain the predicted ASR1 tryptic peptides.

3. Results

3.1. Mapping the DNA-binding activity domain of ASR1

ASR1 possesses a Zn^{2+} -dependent DNA-binding activity [16]. To map the DNA-binding activity of ASR1 we assayed DNA-binding of products of mild acid hydrolysis and truncated ASR1 proteins. The Asp-Pro peptide bond is much more acid labile than a regular peptide bond and mild acid treatment can result in a preferential hydrolysis of this particular bond

[28]. ASR1 has one such acid sensitive peptide bond between residues Asp60-Pro61 (Fig. 2 underlined) and mild acid hydrolysis resulted in two peptides having apparent molecular masses of 7.0 and 6.1 kDa. These correspond, respectively, to the amino (residues 1–60) and carboxy (residues 61–115) terminal domains of ASR1 (Fig. 1). Identity of these peptides was further confirmed by Ni-agarose chromatography: The N-terminal peptide containing the penta His_{6–10} sequence was retained on the Ni-agarose column whereas the C-terminal polypeptide did not bind this matrix (not shown). South-western DNA-binding assays indicate that the carboxy-terminal domain of ASR1 containing residues 61–115 has a zinc-dependent DNA-binding activity, whereas the amino-terminal sequence (residues 1–60) does not (Fig. 1). To further map the amino acid residues involved in DNA-binding activity, a series of protein deletions were prepared by introducing stop codons at codons 105, 97, 87, 77, 69 and 61. This yielded the ASR1 Δ 105–115, ASR1 Δ 97–115, ASR1 Δ 87–115, ASR1 Δ 77–115, ASR1 Δ 69–115 and ASR1 Δ 61–115 truncated polypeptides, respectively (Fig. 2A). Non-tagged truncated proteins were expressed in *E. coli*, purified on Ni-NTA columns by making use of their divalent metal binding activity (Fig. 2B, see also [16]), and used for DNA-binding assays (Fig. 2C). The DNA-binding capacity of the truncated proteins falls into four subgroups: maximal activity was obtained for full-length ASR1 and ASR1 Δ 105–115. ASR1 Δ 77–115 and ASR1 Δ 69–115 retained almost 50% of the binding capacity. On the other hand, ASR1 Δ 96–115 and ASR1 Δ 87–115 had about 25% of the binding activity of the full-length protein, and ASR1 Δ 61–115 had non-significant DNA-binding activity. In all cases the DNA-binding activity was zinc-dependent.

3.2. Zn²⁺ binding by ASR1

MALDI-TOF-MS can be used to study the association of small peptides with metal ions [33]. We applied this approach for the study of Zn²⁺ binding to the full length, 115 amino acid ASR1. When analyzed in DHB or HCCA matrices, prepared by dissolving the matrix in an aqueous solution containing 30–70% acetonitrile and 0.1% TFA, we observed a single 13,127 Da peak corresponding to ASR1 protein (Fig. 3A). Since these matrices are acidic, they very likely cause protein denaturation and in the release any bound ions. Non-acidic aqueous matrices were therefore tested. Purified ASR1 was analyzed by MALDI-TOF-MS using either a THAP matrix or a modified preparation of the HCCA matrix in a saturated (1:1, v:v) 1 M ammonium bicarbonate (pH 8)/ethanol [30]. Using these non-acidic matrices an additional minor peak, corresponding to ASR1 containing one zinc ion (13,127 + 65 Da), was detected (Fig. 3B). The THAP matrix yielded sharper peaks than the aqueous HCCA matrix, and thus was chosen for further studies. To assay the Zn²⁺ binding activity, we analyzed the ion content of ASR1 titrated with different molar equivalents of Zn²⁺ (Fig. 3C–F). Higher zinc concentrations interfered with the MALDI-TOF-MS analysis (not shown). Addition of zinc did not change the pH of the matrix. In all cases, three peaks were observed corresponding to the ion free

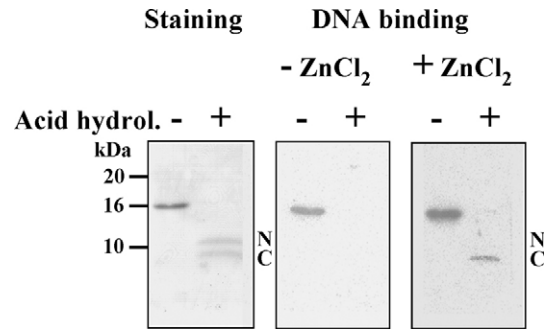


Fig. 1. Mapping of the DNA-binding domain by mild acid hydrolysis of ASR1. Full size (–) and mild acid hydrolyzed ASR1 (+) were resolved on SDS-PAGE and blotted onto nitrocellulose membrane. Proteins were detected by Ponceau S staining (left). Membranes were incubated with radiolabeled dsDNA containing ASR1 preferred binding site (TCCCCA) in the absence (center) or presence of 0.6 mM ZnCl₂ (right). DNA-binding was detected by autoradiography of membranes washed with binding buffer.

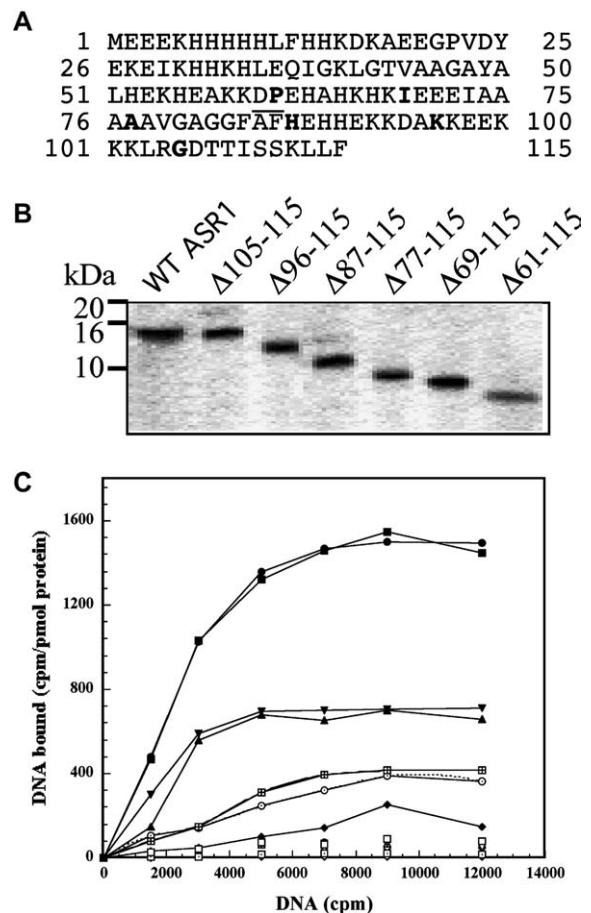


Fig. 2. DNA-binding activity of truncated ASR1 proteins.

A. Truncated ASR1 mutants were obtained by mutating the codons encoding the amino acid residues shown in bold to stop codons. The acid hypersensitive DP peptide bond is underlined. B. Purified truncated proteins were resolved on SDS-PAGE and stained with Coomassie blue. C. DNA-binding activity of WT and truncated ASR1 proteins. DNA-binding was assayed by filter trapping of the protein-radiolabeled DNA complexes. \circ , \bullet , wt ASR1; \square , \blacksquare , ASR1 Δ 105–115; \square , \blacksquare , ASR1 Δ 96–115; \times , \otimes , ASR1 Δ 87–115; \square , \blacktriangledown , ASR1 Δ 77–115; Δ , \blacktriangle , ASR1 Δ 69–115; \diamond , \square , ASR1 Δ 61–115. Empty symbols, binding mix without added zinc. Filled symbols, binding mix contained 0.6 mM ZnCl₂.

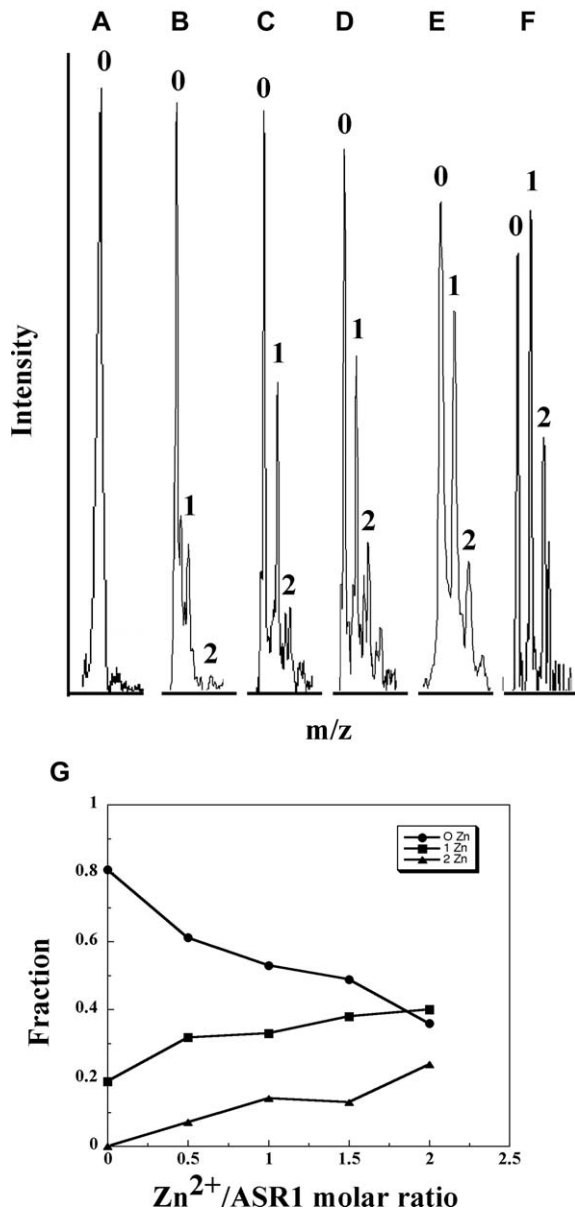


Fig. 3. MALDI-TOF-MS analysis for the binding of Zn²⁺ by ASR1. Full size purified ASR1 was dialyzed against 20 mM Hepes–NaOH pH 7.5. Forty microliters of samples containing 1.2 μg ASR1 were supplemented with A and B, 0; C, 2.5; D, 5; E, 7.5; F, 10 μM ZnCl₂. Mixes were incubated for 20 min at 25 °C and mixed with equal volume of matrices containing (A), 2,5 DHB acid in 33% (v/v) acetonitrile 0.066% TFA, or (B–F), THAP in 50% ethanol 0.5 M ammonium bicarbonate pH 8. Samples were spotted and analyzed by MALDI-TOF-MS. (G) Quantification of mass spectra shown in panels A–F. ●, ■, ▲, 0, 1 or 2 bound Zn²⁺.

ASR1, the 1:1 Zn²⁺/ASR1 complex at +65 Da and the 2:1 Zn²⁺/ASR1 complex at +130 Da. The relative height of the ion free ASR1 peak decreased and that of the other two peaks increased with the proportion of added Zn²⁺ (Fig. 3G). ASR1 did not bind under similar conditions Mg²⁺, Mn²⁺, Ca²⁺, Cu²⁺ or Ni²⁺ in agreement with the previously reported metal specificity of the Zn²⁺ effect on DNA-binding activity of ASR1 [16]. The free concentration of Zn²⁺ is much smaller than that of the added ZnCl₂ probably due to sequestering of zinc ions by these buffers [34].

3.3. Zinc-binding induce conformational changes

To determine whether zinc-binding induces conformational changes, we compared proteolytic patterns obtained by the incubation of ASR1 with various proteases, in the absence and presence of zinc and DNA. Incubation of ASR1 with a variety of proteases resulted in the generation of a large number of low molecular weight proteolytic products (Fig. 4A). In the presence of zinc, a more limited proteolysis of ASR1 was noted (Fig. 4A) with proteolysis patterns dependent on the concentrations of the zinc. Such effects were already observed at 10 μM ZnCl₂ (Fig. 4B). Zinc-binding also protects ASR1 from endogenous tomato leaf protease activity (Fig. 4C, D), as well as chymotrypsin and proteinase V8 (data not shown). Control experiments indicate that the protective effect of zinc did not result from the inhibitory effect of zinc on the proteases, or from a small pH shift caused by the addition of the zinc solution. Addition of DNA containing the preferred ASR1 binding site did not have any effect on the proteolytic pattern obtained in the absence or presence of zinc. The degree of ASR1 degradation in leaf homogenates was dependent on the incubation time, and could be prevented if zinc was included in the homogenization buffer. Furthermore, proteolysis was stopped and no further degradation was observed after the addition of ZnCl₂ to zinc-less leaf homogenate.

3.4. Mapping the zinc-binding domain

To localize the zinc-binding sites, a limited tryptic digest of purified ASR1 in the absence or presence of added zinc ions was carried out. Tryptic peptides from the digest were analyzed by MALDI-TOF-MS using an acidic matrix. Sixty-eight and 28 peaks were observed in the samples treated in the absence and presence of zinc, respectively (Fig. 5) and protein peaks corresponding to trypsin fragments were identified and ignored (as described in Section 2). The most prominent zinc-protected peak contained a 4972 Da tryptic product corresponding to amino-acid residues 1–40. The two other 2256 and 2714 Da major peaks, correspond to proteolytic fragments 1–17 and 18–40, respectively.

To confirm the zinc-binding activity of the N-terminus of ASR1, we tested zinc-binding of the truncated ASR1 mutants. Analysis of all truncated mutants showed three peaks corresponding to the respective polypeptide containing 0, 1 or 2 bound zinc ions. Fig. 6 demonstrates Zn²⁺ binding by ASR1Δ61–115, the smallest truncated mutant analyzed. This demonstrates that the amino-terminal domain of ASR1 is responsible for binding two zinc ions. In addition to bound zinc ions, we observed two minor peaks 23 and 46 Da heavier than Zn-free or Zn-containing ASR1Δ61–115, corresponding to one and two bound Na⁺, respectively. Protein bound Na⁺ was observed only in the truncated protein, but not in the full-length ASR1 (Fig. 3), and appears to be independent from the binding of Zn²⁺.

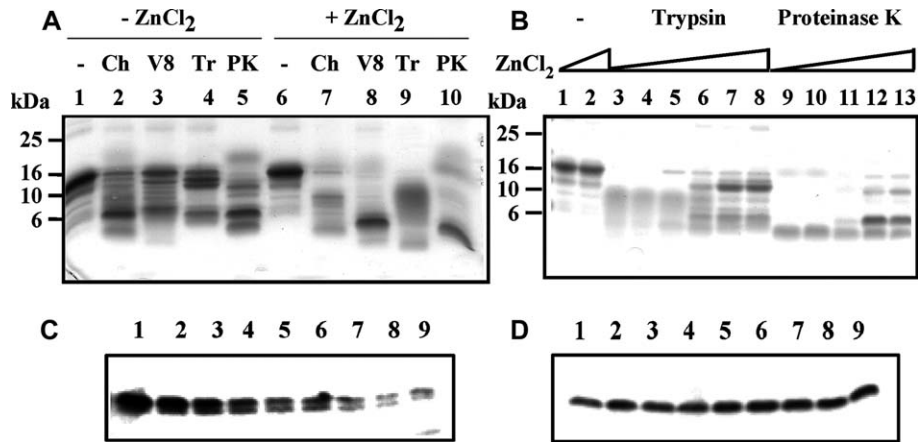


Fig. 4. Zinc-binding decreases proteolytic accessibility of ASR1.

A. Four micrograms of purified ASR1 was incubated with 0.2 μ g trypsin, 12 ng proteinase K, 12 μ g chymotrypsin or 30 ng proteinase V8 for 1 h at 37 °C in the absence or presence of 0 or 0.6 mM $ZnCl_2$. SDS-sample buffer was added, proteins were resolved by SDS-PAGE and stained with Coomassie blue. B. Four micrograms of purified ASR1 was incubated at 37 °C for 1 h with 0.2 μ g trypsin, 12 ng proteinase K in the presence of following concentrations of $ZnCl_2$: 0, lanes 1, 3, 9; 1 μ M, lanes 4, 10; 10 μ M, lanes 5, 11; 50 μ M, lanes 6, 12; 100 μ M, lanes 7, 13 and 200 μ M, lanes 8, 14. Gels were stained with Coomassie blue. C and D. Tomato leaves were homogenized (1:5, w:v) in ice-cold homogenization buffer (25 mM HEPES pH 7.5, 0.5 M sucrose, 10 mM $MgCl_2$, 10 mM β -mercaptoethanol) (panel C) or with homogenization buffer supplemented with 1 mM $ZnCl_2$ (panel D). Homogenates were filtered through four layers of Miracloth (Calbiochem) and incubated on ice. 0.5 ml aliquots were removed (at 1, 2, 5, 10, 15, 20, 30, 45, 60 min after homogenization time, panels B and C, lanes 1–9, respectively) and transferred to pre-chilled tubes containing 10 μ l 50 mM $ZnCl_2$ (panel C) or water (panel D). The tubes were incubated on ice and sulfuric acid (final concentration of 0.2 M) was added to all tubes 60 min after homogenization. Acid soluble proteins were extracted, resolved on SDS-PAGE, and analyzed by Western blot using anti-ASR1 antiserum [16].

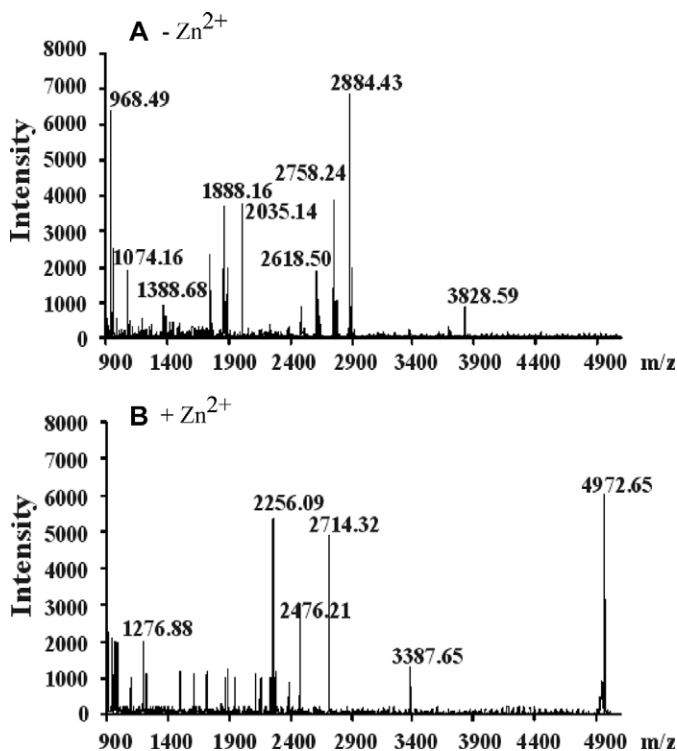


Fig. 5. MALDI-TOF-MS analyses of zinc-dependent tryptic digest products of ASR1.

Full size purified ASR1 was incubated in 20 mM HEPES–NaOH pH 7.5 with trypsin in the presence of 0 (panel A) or 0.6 mM $ZnCl_2$ (panel B). Reaction was quenched after 1 h at 37 °C by the addition of TFA to a final concentration of 2–3% and analyzed by MALDI-TOF-MS as described in Section 2.

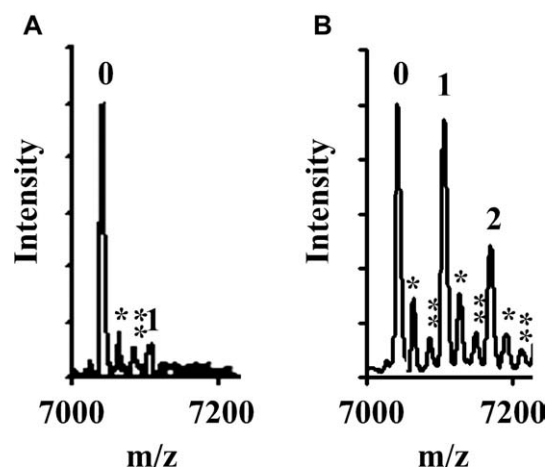


Fig. 6. Zn^{2+} binding by truncated ASR1 Δ 61–115.

Purified ASR1 Δ 61–115 protein was treated as described in Fig. 3 using non-acidic THAP matrix. $ZnCl_2$ concentrations were (A), 0 and (B), 0.6 mM.

4. Discussion

ASR1 possesses a zinc-dependent DNA-binding activity [16]. The amino acid residues or protein domains involved in the binding of DNA, or zinc for that matter, could not be deduced from either a sequence analysis or possible structural homologies. DNA-binding was mapped to the carboxy-terminal residues 61–115 based on products obtained by mild acid hydrolysis (Fig. 1). Furthermore, the DNA-binding activity of the ASR1 carboxy-terminus was zinc dependent, suggesting

that this domain contains a zinc-binding site(s). On the other hand, the high affinity zinc-binding sites detected by MALDI-TOF-MS analyses are at the amino-terminal domain. Using a series of truncation mutants, the amino acid residues involved in DNA-binding were mapped further (Fig. 2). Residues 105–115 do not appear to be involved in zinc-dependent DNA-binding, as their omission does not affect DNA-binding. Deletion of residues 96–115 and 87–115 resulted in a profound decrease (~75%) in DNA-binding activity, albeit still being zinc-dependent. Surprisingly, further deletions of the ASR1 protein (ASR1 Δ 77–115 and ASR1 Δ 69–115) resulted in improved DNA-binding activity (about half that of the wild type ASR1). We propose that this apparently paradoxical observation results from the hydrophobic sequence AAVGAGGF AF at amino acid residues 77–86 of the truncated ASR1 Δ 96–115 and ASR1 Δ 87–115 proteins. These residues may interact with another hydrophobic patch of the truncated proteins, possibly hindering DNA-binding. Removal of these residues results in an increased DNA-binding affinity for the further truncated products ASR1 Δ 77–115 and ASR1 Δ 69–115. As noted with the amino-terminal residues 1–60 obtained by mild acid hydrolysis (Fig. 1), the truncated ASR1 Δ 61–115 protein did not bind DNA (Fig. 2). The smallest fragments that had significant zinc-dependent DNA-binding activity were residues 61–115 (Fig. 1) and 1–68 (Fig. 2) obtained by mild acid hydrolysis and site directed mutagenesis, respectively. These polypeptides overlap in residues 61–68 (PEHAHKHK) suggesting that these residues are the ones involved in the zinc-dependent DNA-binding activity of ASR1.

Zinc containing DNA-binding proteins are common in eukaryotes [18], and the most studied and possibly most abundant are the zinc-finger proteins. In these proteins, zinc is coordinated by four amino acid residues, of which at least two are usually Cys. Since ASR1 lacks any Cys residue, it is unlikely that it is a zinc finger protein, or any other abundant zinc-binding motifs for that matter, found in DNA-binding proteins. Thus, neither the number nor the localization of zinc-binding sites on ASR1 protein can be predicted by comparison to known zinc-binding motifs. Moreover, zinc coordinating residues such as His, Glu or Asp [22] appear in high copies in ASR1 (18, 18 and 5 residues, respectively). Based on the DNA-binding activity and the MALDI-TOF-MS studies, we suggest that ASR1 binds at least three zinc ions: two at the amino-terminal domain and at least one at the DNA-binding domain.

Binding of 2 mol Zn²⁺ per mol of ASR1 polypeptide could be detected in full-length ASR1 using MALDI-TOF-MS with a non-acidic matrix (Fig. 3). Interaction between metal ions and polypeptides was previously shown by MALDI-TOF-MS [30, 34] and in this study we demonstrate zinc-binding by the full-length ASR1. In agreement with the known features of coordination of the residues of His, Asp and Glu with ions of transition metals, no zinc-binding was observed in an acidic matrix (Fig. 3A). Titration of the zinc-binding sites suggested that both zinc ions bind with similar affinities (Fig. 3G). However, it is not clear if there is a sequential binding of the ions at the two zinc-binding sites or whether zinc binds to each site inde-

pendently of the other. Zinc-binding to ASR1 also results in conformational changes as demonstrated by the decrease in accessibility of the protein to proteases (Figs. 4 and 5). The zinc concentrations affecting the accessibility to proteases are in the lower micromolar range (Fig. 4) whereas those required for stimulation of DNA-binding are at least one order of magnitude higher [16], suggesting that these sites are different. These differences in affinity for zinc suggest a physiological role for ASR1 in sensing zinc levels and a possible relation to stress response. This is highlighted by the result that the amino-terminal domain of ASR1 binds two zinc ions (Figs. 5 and 6) and does not possess DNA-binding activity, whereas the central/carboxy-terminus domain is responsible for the zinc-dependent DNA-binding activity of ASR1 (Fig. 1). The affinity determined is in the range of cellular concentration of zinc. For example, in tomato leaf zinc content is 55 mg/kg dry mass [35]. The mass ratio of water to dry weight of irrigated tomato leaf is approximately 6 [36]. Assuming that zinc is evenly distributed in the aqueous phase of the plant it reaches concentration of about 0.15 mM. Upon water- and salt-stress the water content in plant tissues decreases, which results in increasing of solute concentrations including zinc ions. Furthermore, the free concentration of Zn²⁺ in the reaction mixtures is much smaller than that of the added ZnCl₂ probably due to sequestering of zinc ions by these buffers [33].

Zinc-binding sites at the amino-terminal domain of ASR1 were further mapped by protease analysis. Three polypeptides comprising amino acid residues 1–40 and its components 1–17 and 18–40 were obtained after trypsin digestion of ASR1 in the presence of zinc (Fig. 5). These proteolytic fragments were missing if digestion was carried in the absence of added zinc. The zinc-binding domain identified does not have a signature of any of the studied zinc-binding sites [22]. Thus, identifying the amino acid residues involved in zinc-binding site requires further studies.

Acknowledgements

This study was supported by a grant from the Israel Science Foundation awarded to D.B.-Z. and Y.G. We thank Dr. Rodolfo Ghirlando for critical reading of the manuscript.

References

- [1] H. Amitai-Zeigerson, P.A. Scolnik, D. Bar-Zvi, Tomato *Asr1* mRNA and protein are transiently expressed following salt stress, osmotic stress and treatment with abscisic acid, *Plant Sci.* 110 (1995) 205–213.
- [2] N.D. Iusem, D.M. Bartholomew, W.D. Hitz, P.A. Scolnik, Tomato (*Lycopersicon esculantum*) transcript induced by water deficit and ripening, *Plant Physiol.* 102 (1993) 1353–1354.
- [3] H. Amitai-Zeigerson, P.A. Scolnik, D. Bar-Zvi, Genomic nucleotide sequence of tomato *Asr2*, a second member of the stress/ripening-induced *Asr1* gene family, *Plant Physiol.* 106 (1994) 1699–1700.
- [4] M. Rossi, D. Lijavetzky, D. Bernacchi, H.E. Hopp, N. Iusem, *Asr* genes belong to a gene family comprising at least three closely linked loci on chromosome 4 in tomato, *Mol. Gen. Genet.* 252 (1996) 489–492.
- [5] F. Carrari, A.R. Fernie, N.D. Iusem, Heard it through the grapevine? ABA and sugar cross-talk: the ASR story, *Trends Plant Sci.* 9 (2004) 57–59.

- [6] H. Wang, S. Miyazaki, K. Kawai, M. Deyholos, D.W. Galbraith, H. J. Bonhert, Temporal progression of gene expression responses to salt shock in maize roots, *Plant Mol. Biol.* 52 (2003) 873–891.
- [7] S. Kawasaki, C. Borchert, M. Deyholos, H. Wang, S. Brazille, K. Kawai, D. Galbraith, H.J. Bohnert, Gene expression profiles during the initial phase of salt stress in rice, *Plant Cell* 13 (2001) 889–905.
- [8] A. Gilad, H. Amitai-Zeigerson, D. Bar-Zvi, ASR1 a tomato water-stress regulated gene: genomic organization, developmental regulation and DNA-binding activity, *Acta Hort.* 447 (1997) 447–453.
- [9] S.H. Hong, I.-J. Kim, D.C. Yang, W.-I.I. Chung, Characterization of an abscisic acid responsive gene homologue from *Cucumis melo*, *J. Exp. Bot.* 53 (2002) 2271–2272.
- [10] C.S. Wang, Y.E. Liau, J.C. Huang, T.D. Wu, C.C. Su, C.H. Lin, Characterization of a desiccation-related protein in lily pollen during development and stress, *Plant Cell Physiol.* 39 (1998) 1307–1314.
- [11] D. Silhavy, G. Hutvagner, E. Barta, Z. Banfalvi, Isolation and characterization of a water-stress inducible cDNA clone from *Solanum chacoense*, *Plant Mol. Biol.* 27 (1995) 587–595.
- [12] S. Chang, J.D. Puryear, M.A.D.L. Dias, E.A. Funkhauser, R.G. Newton, J. Cairney, Gene expression under water deficit in loblolly pine (*Pinus taeda* L.): isolation and characterization of cDNA clones, *Physiol. Plant.* 97 (1996) 139–148.
- [13] C. Canel, J.N. Bailey-Serres, M.L. Roose, Pummelo fruit transcript homologous to ripening-induced gene, *Plant Physiol.* 108 (1995) 1323–1324.
- [14] A. Itai, K. Tanabe, F. Tamura, T. Tanaka, Isolation of cDNA clones corresponding to genes expressed during fruit ripening in Japanese pear (*Pyrus pyrifolia* Nakai): involvement of the ethylene signal transduction pathway in their expression, *J. Exp. Bot.* 51 (2000) 1163–1166.
- [15] B. Cakir, A. Agasse, C. Gaillard, A. Saumonneau, S. Delrot, R. Atanassova, A grape ASR protein involved in sugar and abscisic acid signaling, *Plant Cell* 15 (2003) 2165–2180.
- [16] Y. Kalifa, A. Gilad, Z. Konrad, M. Zaccai, P.A. Scolnik, D. Bar-Zvi, The water- and salt-stress regulated *Asr1* gene encodes a zinc-dependent DNA-binding protein, *Biochem. J.* 381 (2004) 373–378.
- [17] Y. Kalifa, E. Perlson, A. Gilad, Z. Konrad, P.A. Scolnik, D. Bar-Zvi, Over-expression of the water and salt stress-regulated *Asr1* gene confers an increased salt tolerance, *Plant Cell Environ.* 27 (2004) 1459–1468.
- [18] N.M. Luscombe, S.E. Austin, H.M. Berman, J.M. Thornton, An overview of the structure of protein-DNA complexes, *Genome Biol.* 1 (2000) 001.1–001.37.
- [19] R.G. Brennan, B.W. Matthews, The HTH DNA-binding motif, *J. Biol. Chem.* 264 (1989) 1903–1906.
- [20] W.H. Landschulz, P.F. Johnson, S.L. McKnight, The Leucine zipper—a hypothetical structure common to a new class of DNA-binding proteins, *Science* 240 (1989) 1759–1764.
- [21] A.R. Ferre-d'Amare, G.C. Prendergast, E.B. Ziff, E.B.S.K. Burley, Recognition by Max of its cognate DNA through a dimeric b/HLH/Z domain, *Nature* 363 (1993) 38–45.
- [22] D.S. Auld, Zinc coordination sphere in biochemical zinc sites, *Biomaterials* 14 (2001) 271–313.
- [23] G.H. Jacob, Determination of the base recognition positions of zinc finger from sequence analysis, *EMBO J.* 11 (1992) 4507–4517.
- [24] R.K. Patient, J.D. McGhee, The GATA family (vertebrates and invertebrates), *Curr. Opin. Genet. Dev.* 12 (2002) 416–422.
- [25] L.P. Freedman, B.F. Luisi, On the mechanism of DNA-binding by nuclear hormone receptors—a structural and functional perspective, *J. Cell. Biochem.* 51 (1993) 140–150.
- [26] Y. Cho, S. Gorina, P.D. Jeffery, N.P. Pavletich, Crystal structure of a p53 tumor suppressor–DNA complex: understanding tumorigenic mutations, *Science* 265 (1994) 346–355.
- [27] R. Marmorstein, M. Carey, M. Ptashne, S.C. Harrison, DNA recognition by GAL4: structure of a proteins–DNA complex, *Nature* 356 (1992) 408–414.
- [28] G.E. Tarr, Manual Edman sequencing system, in: J.E. Shively (Ed.), *Methods of Protein Microcharacterization: A Practical Handbook*, Human Press, USA, Clifton, NJ, 1986, pp. 155–194.
- [29] S.P. Fling, D.S. Gregerson, Peptide and protein molecular weight determination by electrophoresis using high-molarity tris buffer system without urea, *Anal. Biochem.* 155 (1986) 83–88.
- [30] A.S. Woods, J.C. Buchsbaum, T.A. Worrall, J.M. Berg, R.J. Cotter, Matrix-assisted laser desorption/ionization of noncovalently bound compounds, *Anal. Chem.* 6 (1995) 4462–4465.
- [31] F. Landry, C.R. Lombardo, J.W. Smith, A method for application of samples to matrix-assisted laser desorption ionization time-of-flight targets that enhances peptide detection, *Anal. Biochem.* 279 (2000) 1–8.
- [32] R. Westermeier, T. Naven, Calibration of the MALDI-TOF-MS, in: R. Westermeier, T. Naven (Eds.), *Proteomics in Practice. A Laboratory Manual of Proteome Analysis*, Wiley-VCH, Germany, 2002, pp. 273–275.
- [33] R.M.C. Dawson, D.C. Elliott, W.H. Elliott, K.M. Jones, *Data for Biochemical Research*, third ed, Oxford Press, Oxford, UK, 1986.
- [34] B. Salih, C. Masselon, R. Zenobi, Matrix-assisted laser desorption/ionization mass spectrometry of noncovalent protein transition metal ion complexes, *J. Mass Spect.* 33 (1998) 994–1002.
- [35] P. Castaldi, P. Melis, Growth and yield characteristics and heavy metal content on tomato grown in different growing media, *Commun. Soil Sci. Plant Anal.* 35 (2004) 85–98.
- [36] T.-H. Hsieh, J.-T. Lee, Y.-y. Chang, M.-T. Chan, Tomato plants ectopically expressing *Arabidopsis* CBF1 show enhanced resistance to water deficit stress, *Plant Physiol.* 130 (2002) 618–626.